

**Supplementary information**

# Effect of piperidinium structure on anion-exchange membranes for applications in alkaline water electrolysis cells

Yoshihiro Ozawa,<sup>a</sup> Toshio Iwataki,<sup>b</sup> Makoto Uchida,<sup>b</sup> Katsuyoshi Kakinuma<sup>bc</sup> and Kenji Miyatake<sup>\*bcd</sup>

<sup>a</sup>Interdisciplinary Graduate School of Medicine and Engineering, University of Yamanashi, 4 Takeda, Kofu, Yamanashi 400-8510, Japan

<sup>b</sup>Hydrogen and Fuel Cell Nanomaterials Center, University of Yamanashi, 6-43 Miyamae-cho, Kofu 400-0021, Japan

<sup>c</sup>Clean Energy Research Center, University of Yamanashi, 4 Takeda, Kofu, Yamanashi 400-8510, Japan

<sup>d</sup>Department of Applied Chemistry, Waseda University, Tokyo 169-8555, Japan

\*Corresponding author

E-mail addresses: [miyatake@yamanashi.ac.jp](mailto:miyatake@yamanashi.ac.jp) (K. Miyatake)

Keywords: anion exchange membranes, ionomers, piperidinium groups, alkaline water electrolysis cells

## Materials

Piperidine (> 99.0%, TCI), 4-methylpiperidine (> 98.0%, TCI), 3,5-dimethylpiperidine (cis- and trans- mixture) (> 98.0%, TCI), 4-(trifluoromethyl)piperidine (> 97.0%, TCI), 1-(*tert*-butoxycarbonyl)-4-piperidinemethanol (> 98.0%, TCI), tetrahydrofuran (THF) (dehydrated, stabilizer free, > 99.5%, Kanto Chemical), potassium carbonate (> 99.0%, Kanto Chemical), sodium chloride (> 99.0%, Kanto Chemical), iodine (> 99.8%, Kanto Chemical), triphenylphosphine (> 95.0%, TCI), imidazole (> 98.0%, TCI), tetrabutylammonium bromide (> 98.0%, TCI), sodium hydroxide (> 97.0%, Kanto Chemical), dimethyl sulfoxide (DMSO) (> 99.0%, Kanto Chemical), ethyl acetate (> 99.3%, Kanto Chemical), chloroform (> 99.0%, Kanto Chemical), hexane (> 95.0%, Kanto Chemical), methanol (> 99.8%, Kanto Chemical), sodium sulfate (> 98.5%, Kanto Chemical), hydrochloric acid (35-37%, Kanto Chemical), potassium hydroxide (> 86.0%, Kanto Chemical), 2,2'-bipyridyl (> 99.0%, TCI), bis(1,5-cyclooctadiene)nickel(0) (Ni(cod)<sub>2</sub>) (> 95.0%, Kanto Chemical), and dimethyl sulfate (> 99%, Kanto Chemical) were used as received. N,N-Dimethylacetamide (DMAc) (> 99.0%, Kanto Chemical) was purified with a solvent refining apparatus before use. 2,7-Dichlorofluorene, 2,7-dichloro-9,9-bis(6-bromohexyl)-9*H*-fluorene and monomer **6** were synthesized according to our previous work.<sup>26</sup>

### Synthesis of 1'1-((2,7-dichloro-9*H*-fluorene-9,9-diyl)bis(hexane-6,1-diyl))dipiperidine (monomer **1**, Scheme S1)

2,7-Dichloro-9,9-bis(6-bromohexyl)-9*H*-fluorene (3.0 g, 5.35 mmol), piperidine (9.1 g, 107 mmol) and THF (30.0 mL) were added to a 100 mL round-bottom flask and reacted at 40 °C for 48 h under nitrogen atmosphere. After the reaction, the mixture was neutralized with 0.1 M potassium carbonate aqueous solution (50 mL). The organic layer was extracted with hexane. The combined organic layer was dehydrated with sodium

sulfate, filtered, and evaporated to obtain 1'1'-((2,7-dichloro-9*H*-fluorene-9,9-diyl)bis(hexane-6,1-diyl))dipiperidine as a pale yellow oil (3.2 g, quant).

**Synthesis of 1'1'-((2,7-dichloro-9*H*-fluorene-9,9-diyl)bis(hexane-6,1-diyl))bis(4-methylpiperidine) (monomer 2, Scheme S1)**

Monomer 2 was obtained in the similar manner to the monomer 1 as a pale yellow oil (3.2 g, quant).

**Synthesis of 1'1'-((2,7-dichloro-9*H*-fluorene-9,9-diyl)bis(hexane-6,1-diyl))bis(3,5-diethylpiperidine) (monomer 3, Scheme S1)**

Monomer 3 was prepared in the similar manner to the monomer 1. Silica gel column chromatography (eluent: AcOEt) was carried out to obtain pure 3 as a colorless transparent oil (1.1 g, 32% yield).

**Synthesis of 1'1'-((2,7-dichloro-9*H*-fluorene-9,9-diyl)bis(hexane-6,1-diyl))bis(4-(trifluoromethyl)piperidine) (monomer 4, Scheme S1)**

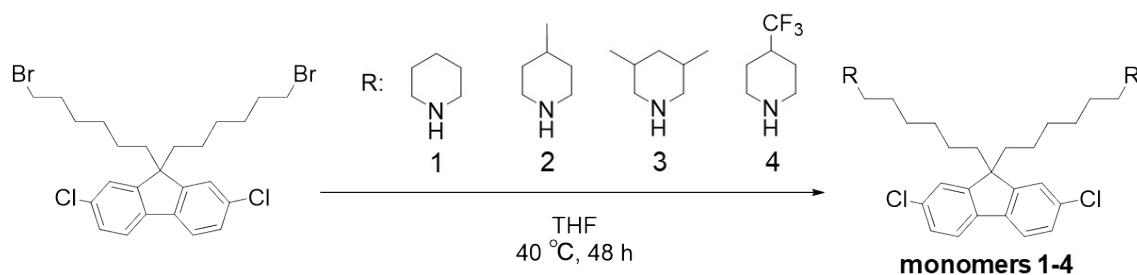
Monomer 4 was prepared in the similar manner to the monomer 1. Silica gel chromatography (eluent: AcOEt) was carried out to obtain pure 4 as a colorless transparent oil (1.4 g, 90% yield).

**Synthesis of di-*tert*-butyl 4,4'-((2,7-dichloro-9*H*-fluorene-9,9-diyl)bis(methylene))bis(piperidine-1-carboxylate) (monomer 5, Scheme S2)**

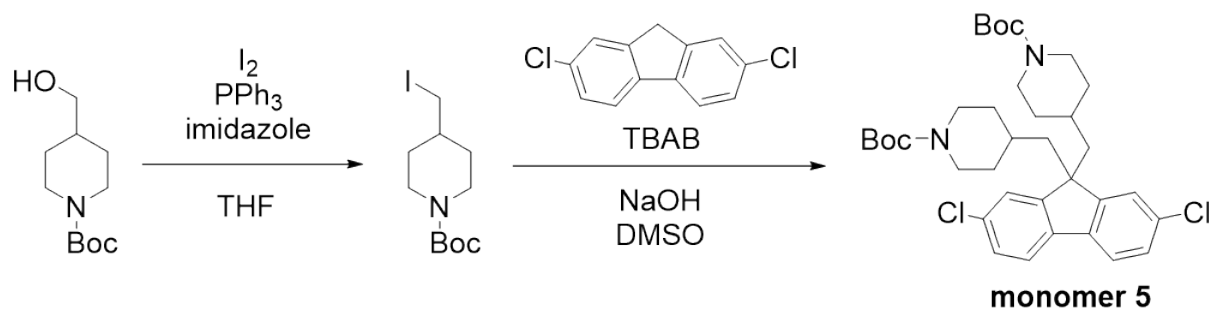
1-(*tert*-Butoxycarbonyl)-4-piperidinemethanol (5.0 g, 23.2 mmol), imidazole (1.4 g, 20.6 mmol), and triphenylphosphine (7.3 g, 27.8 mmol) were mixed in THF (30 mL) and stirred for 0.5 h at 0 °C in nitrogen atmosphere. To the mixture, iodine (7.2 g, 28.4 mmol) dissolved in THF (20 mL) was added and the mixture was reacted at room temperature for 3.5 h. The reaction was quenched with NaHSO<sub>3</sub> (3.0 g, 28.4 mmol). The product was

extracted with ethyl acetate, and combined organic layer was washed with brine. The organic layer was dehydrated with sodium sulfate and evaporated. The crude product was purified by silica gel column chromatography (eluent: hexane/AcOEt = 9/1) to obtain 1-(*tert*-butoxycarbonyl)-4-piperidinemethanol as a colorless transparent oil (5.8 g, 77% yield).

2,7-Dichlorofluorene (1.4 g, 5.93 mmol), 1-(*tert*-butoxycarbonyl)-4-piperidinemethanol (5.8 g, 17.8 mmol), and tetrabutylammonium bromide (0.5 g, 1.55 mmol) were dissolved in DMSO (13 mL) in a 100 mL round-bottom flask. 50 wt% NaOH aqueous solution (3 mL) was added, and the mixture was stirred at room temperature for 24 h. The reaction was quenched by adding excess deionized water. The product was extracted with ethyl acetate, and combined organic layer was washed with brine. The organic layer was dehydrated with sodium sulfate and evaporated. The crude product was purified by silica gel column chromatography (eluent: hexane/AcOEt = 10/1→8/1→4/1) to obtain monomer **5** as a slightly reddish white solid (2.6 g, 70% yield).



Scheme S1 Synthesis of monomers 1-4.



Scheme S2 Synthesis of monomer 5.

## Measurements

$^1\text{H}$  and  $^{19}\text{F}$  NMR spectra were obtained on a JEOL JNM-ECA/ECX500 using deuterated chloroform ( $\text{CDCl}_3$ ), 1,1,2,2-tetrachloroethane ( $\text{TCE-}d_2$ ), or dimethylsulfoxide ( $\text{DMSO-}d_6$ ). Tetramethylsilane (TMS) or the solvent was used as an internal reference. Molecular weight was measured with gel permeation chromatography (GPC) equipped with a Shodex K-805 L column and a Jasco UV 2077 detector (270 nm) with  $\text{CHCl}_3$  containing 0.03 M triethylamine as eluent. Molecular weight was calibrated with standard polystyrene samples (ranged from  $M_n = 1.26$  to 423 kDa, 10 samples). FT-IR was obtained on a Nicolet 6700 (Thermo Fisher Scientific Inc.).

Ion exchange capacity (IEC) was determined by titration. A membrane sample (ca. 20 mg) in chloride ion form was immersed in 0.2 M  $\text{NaNO}_3$  aqueous solution (12.5 mL) at r.t. for 24 h. The amount of chloride ions released from the membrane was titrated with 0.01 M  $\text{AgNO}_3$  using  $\text{K}_2\text{CrO}_4$  as an indicator and  $\text{NaHCO}_3$  as a pH adjuster.

Hydroxide ion conductivity of the membranes was measured in degassed, deionized water ( $> 18 \text{ M}\Omega$ ) at 30, 40, 60, and 80  $^\circ\text{C}$  using a 4-probe conductivity cell attached with an AC impedance apparatus (Solartron 1255B, Solartron Inc.). Ion conducting resistance ( $R$  ( $\Omega$ )) was determined from the impedance plot obtained in the frequency range from 1 to  $10^5$  Hz. The hydroxide ion conductivity ( $\sigma$ ) was calculated from the equation,  $\sigma = l/AR$ ,

where  $A$  ( $\text{cm}^2$ ) and  $l$  (cm) are the cross-section area of the membrane and the distance between two reference electrodes, respectively.

Water uptake was calculated using the following equation: Water uptake (%) =  $(W_w - W_d) / W_d \times 100$ , where  $W_w$  is the wet weight and  $W_d$  the dry weight (dried in a vacuum oven at 50 °C overnight) of the membrane.

Swelling ratio was calculated using the following equation: Swelling ratio (%) =  $(L_w - L_D) / L_D \times 100$ , where  $L_w$  is the wet length of the membrane ( $\text{OH}^-$  form) and  $L_D$  is dry length of the membrane ( $\text{MeSO}_4^-$  form, dried in a vacuum oven at 50 °C overnight). The test sample was cut to  $1 \times 4 \text{ cm}^2$ , and the change in the longer side direction (ca. 4 cm) of the membrane with a small error was measured.

Scanning electron microscopy (SEM) was carried out using a Hitachi SU3500.

Dynamic mechanical analysis (DMA) was carried out with an ITK DVA-225 dynamic viscoelastic analyzer. Temperature dependence of the storage modulus ( $E'$  (Pa)), loss modulus ( $E''$  (Pa)), and  $\tan \delta$  ( $= E''/E'$ ) at 60% RH and 10 Hz was measured for the membranes in chloride ion forms ( $5 \times 30 \text{ mm}$ ) between r.t. and 100 °C at a heating rate of  $1 \text{ }^\circ\text{C min}^{-1}$ . Humidity dependence of  $E'$ ,  $E''$ , and  $\tan \delta$  at 80 °C and 10 Hz was also measured between 0% and 90% RH at a humidifying rate of  $1\% \text{ RH min}^{-1}$ .

Tensile strength test was carried out with a Shimadzu universal testing instrument Autograph AGS-J500N equipped with a temperature and humidity controllable chamber. A membrane sample in chloride ion form was cut into a dumbbell shape ( $35 \times 6 \text{ mm}$  (total) and  $12 \times 2 \text{ mm}$  (test area)). Stress strain curves were obtained at 80 °C and 60% RH at a stretching rate of  $10 \text{ mm min}^{-1}$  after equilibrating the membrane at least for 3 h.

Alkaline stability of the membranes was performed in 8 M KOH aqueous solution at 80 °C. The alkaline solution was replaced with fresh KOH solution approximately every 168 hours to remove the decomposition products. The hydroxide ion conductivity was

monitored in degassed water at 40 °C as a function of the testing time. Post-test analysis was performed by NMR spectra and tensile tests.

Table S1 Weight and IEC value of the membranes and their standard deviations

| sample  | Membrane weight (mg) <sup>a</sup> |      |      | IEC (meq. g <sup>-1</sup> ) |      |      | IEC <sup>b</sup> (meq. g <sup>-1</sup> ) | Standard deviation of IEC value (meq. g <sup>-1</sup> ) |
|---------|-----------------------------------|------|------|-----------------------------|------|------|--|---|
|         | 1                                 | 2    | 3    | 1                           | 2    | 3    |  |   |
| QBP-1   | 16.6                              | 20.6 | 19.4 | 1.97                        | 1.94 | 1.90 | 1.94                                     | 0.03  |
| QBP-2   | 20.6                              | 18.6 | 20.1 | 1.99                        | 1.93 | 1.96 | 1.96                                     | 0.02  |
| QBP-3   | 15.8                              | 18.0 | 18.7 | 2.01                        | 1.93 | 1.97 | 1.97                                     | 0.03  |
| QBP-4   | 20.6                              | 20.0 | 21.3 | 1.56                        | 1.51 | 1.48 | 1.52                                     | 0.03  |
| QBM-2.1 | 13.4                              | 16.1 | 13.7 | 1.98                        | 1.94 | 1.98 | 1.97                                     | 0.02  |
| QBM-2.7 | 18.6                              | 14.1 | 15.5 | 2.49                        | 2.46 | 2.48 | 2.48                                     | 0.01  |
| QBM-3.2 | 11.8                              | 15.9 | 12.7 | 2.97                        | 2.97 | 3.01 | 2.98                                     | 0.02  |

<sup>a</sup>Membrane weight was for the dry samples (Cl<sup>-</sup> form) after vacuum dried for 24 h.

<sup>b</sup>Averaged IEC values for three measurements.

Table S2 Standard deviation of water uptake, swelling ratio, OH<sup>-</sup> conductivity and

IEC<sub>volume</sub> and the membrane thickness of the sample used for each measurement.

| sample  | Water uptake (%) @r.t.          | Swelling ratio (%) @r.t.        | OH <sup>-</sup> conductivity (mS cm <sup>-1</sup> ) @30 °C |                                      | IEC <sub>volume</sub> (meq. cm <sup>-3</sup> ) @30 °C |                                      |
|---------|---------------------------------|---------------------------------|--|--------------------------------------|---|--------------------------------------|
|         | Standard deviation <sup>a</sup> | Standard deviation <sup>b</sup> | Standard deviation <sup>c</sup>                            | Membrane thickness (μm) <sup>d</sup> | Standard deviation <sup>e</sup>                       | Membrane thickness (μm) <sup>f</sup> |
| QBP-1   | 1.63                            | 1.16                            | 1.59   | 39                                   | 0.06  | 41                                   |
| QBP-2   | 5.73                            | 0.51                            | 8.94   | 48                                   | 0.16  | 43                                   |
| QBP-3   | 5.73                            | 0.12                            | 1.19   | 24                                   | 0.17  | 39                                   |
| QBP-4   | 6.34                            | 0.00                            | 0.85   | 41                                   | 0.09  | 36                                   |
| QBM-2.1 | 14.70                           | 0.59                            | 0.91   | 31                                   | 0.07  | 26                                   |
| QBM-2.7 | 17.21                           | 0.51                            | 1.32   | 60                                   | 0.05  | 34                                   |
| QBM-3.2 | 243.70                          | N/A                             | 2.44   | 79                                   | 0.01  | 49                                   |

<sup>a</sup>Standard deviation of water uptake for three measurements. <sup>b</sup>Standard deviation of swelling ratio for three measurements. <sup>c</sup>Standard deviation of OH<sup>-</sup> conductivity measured for three measurements. <sup>d</sup>Averaged thickness (OH<sup>-</sup> form) for wet samples. <sup>e</sup>Standard deviation of IEC<sub>volume</sub> for three measurements. <sup>f</sup>Averaged thickness (MeSO<sub>4</sub><sup>-</sup> form) for dry samples.

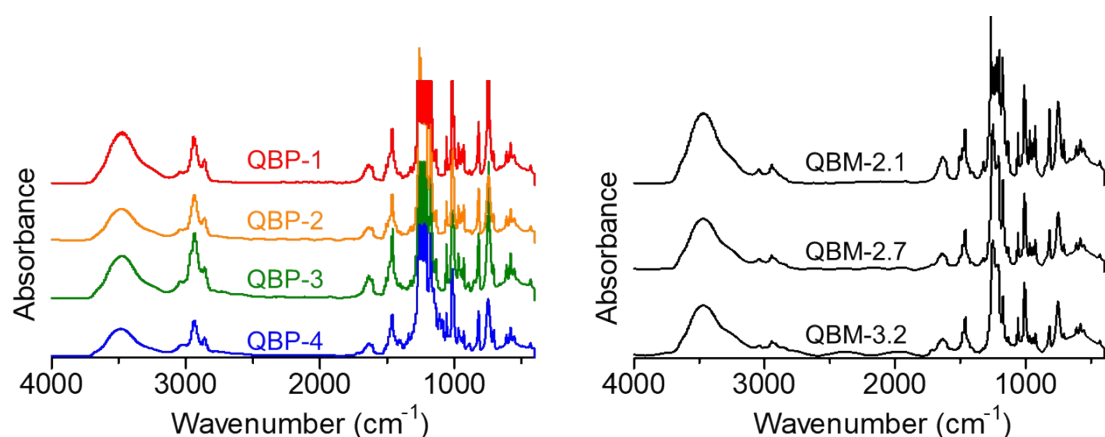


Fig. S1 IR spectra of QBP-R(1-4), QBM-2.1, QBM-2.7 and QBM-3.2 membranes (in MeSO<sub>4</sub><sup>-</sup> form).



Fig. S2 Photos of of QBP-R(1-4), QBM-2.1, QBM-2.7 and QBM-3.2 membranes (in  $\text{MeSO}_4^-$  form).

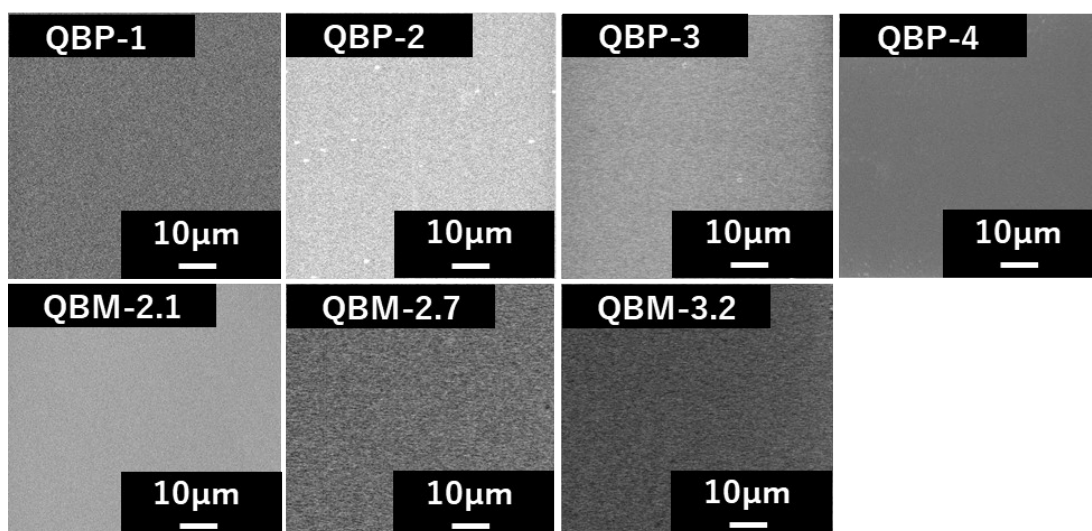


Fig. S3 SEM images (surface) of QBP-R(1-4), QBM-2.1, QBM-2.7 and QBM-3.2 membranes (in  $\text{MeSO}_4^-$  form).

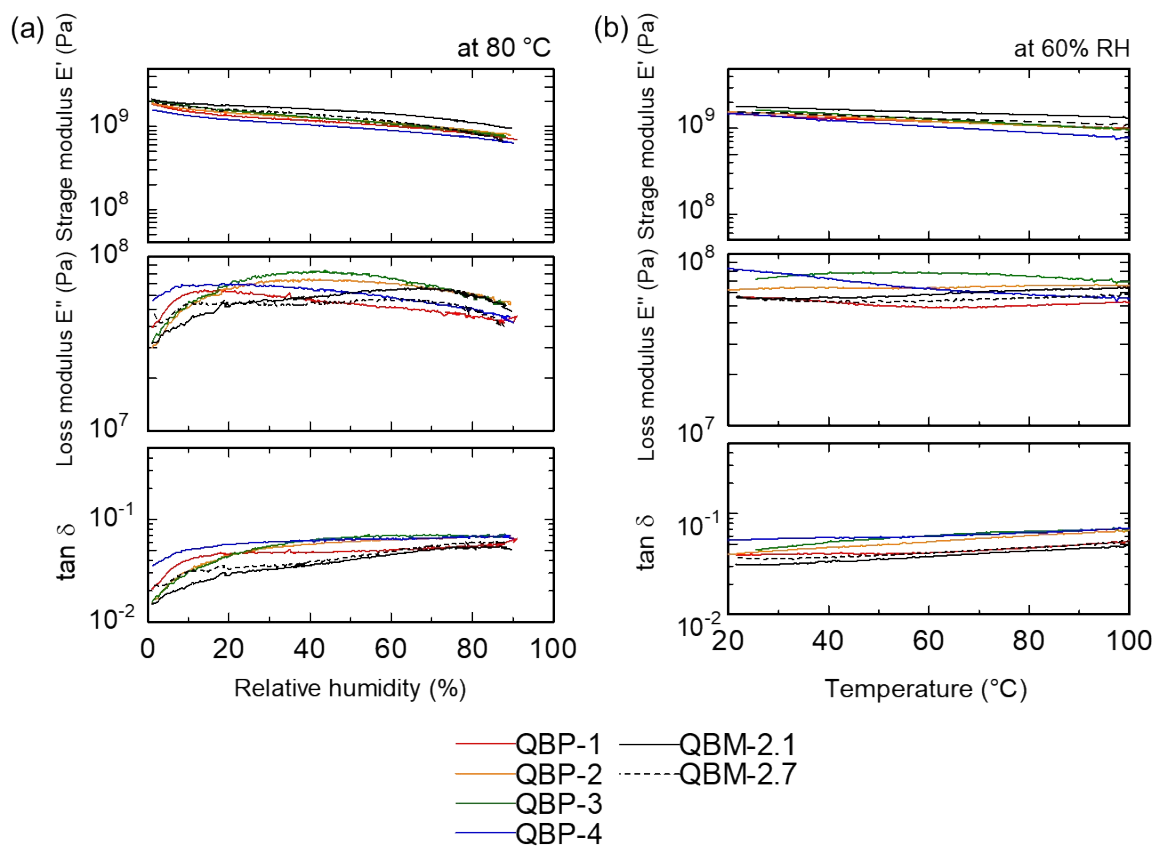


Fig. S4 DMA curves of QBP-R(1-4) (solid lines), QBM-2.1 (solid line) and QBM-2.7 (dashed line) membranes (in  $\text{Cl}^-$  form). (a) Humidity dependence at 80 °C and (b) temperature dependence at 60% RH.

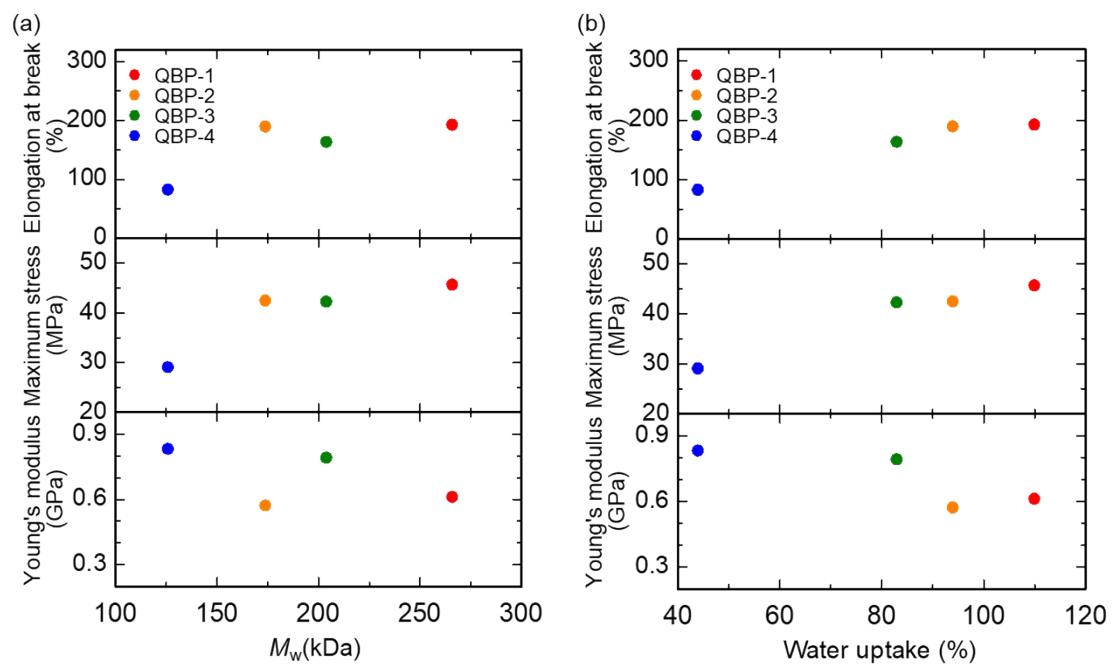


Fig. S5 Mechanical properties of QBP-R(1-4) membranes as a function of (a) weight average molecular weight ( $M_w$ ) and (b) water uptake.

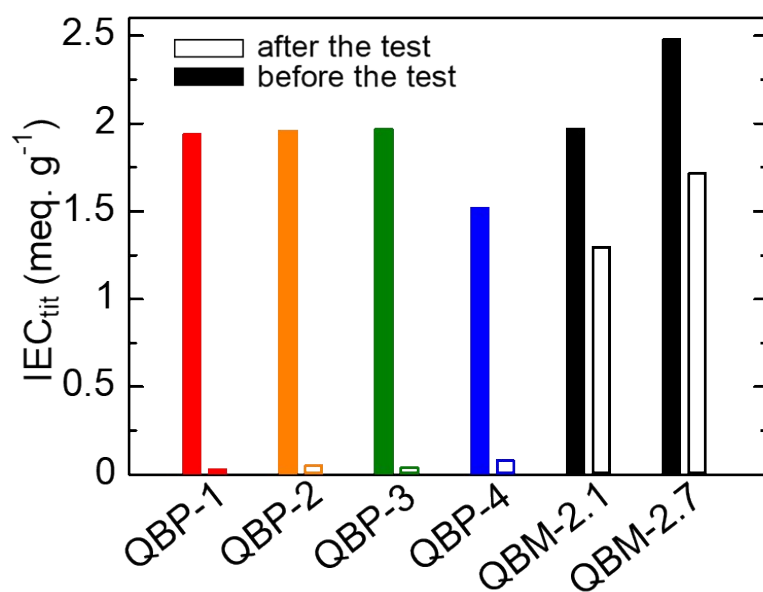


Fig. S6 IEC values of the titrated QBP-R(1-4) and QBM-X(2.1 and 2.7) membranes before/after alkaline stability test (in 8 M KOH at 80 °C). The post-test IEC values of the QBP-R membranes were titrated at the time when the conductivity was almost lost, which were 810 (QBP-1), 324 (QBP-2), 291 (QBP-3), 129 h (QBP-4). For QBM-X membranes, the test was terminated at 1000 hours.

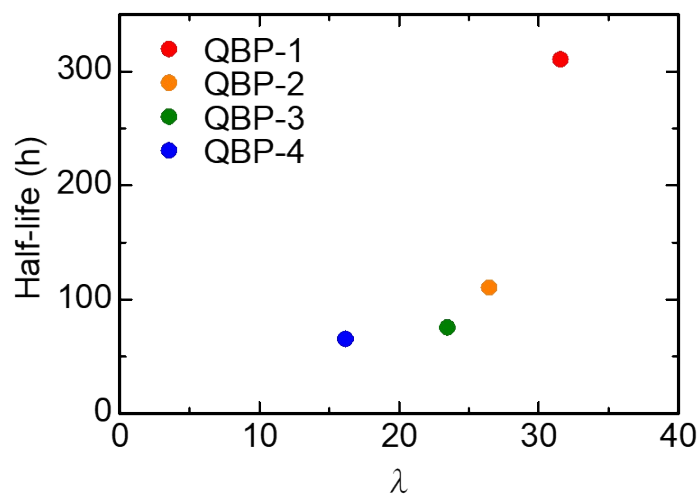


Fig. S7 Half-life ( $\text{OH}^-$  conductivity) of QBP-R(1-4) membranes as a function of hydration number during the alkaline stability test (in 8 M KOH at 80 °C).

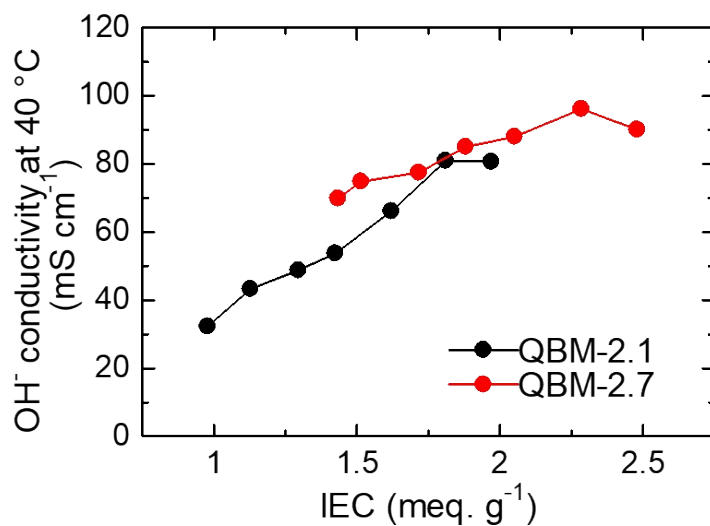


Fig. S8  $\text{OH}^-$  conductivity of QBM-2.1 and QBM-2.7 membranes as a function of IEC values during the alkaline stability test (in 8 M KOH at 80 °C).

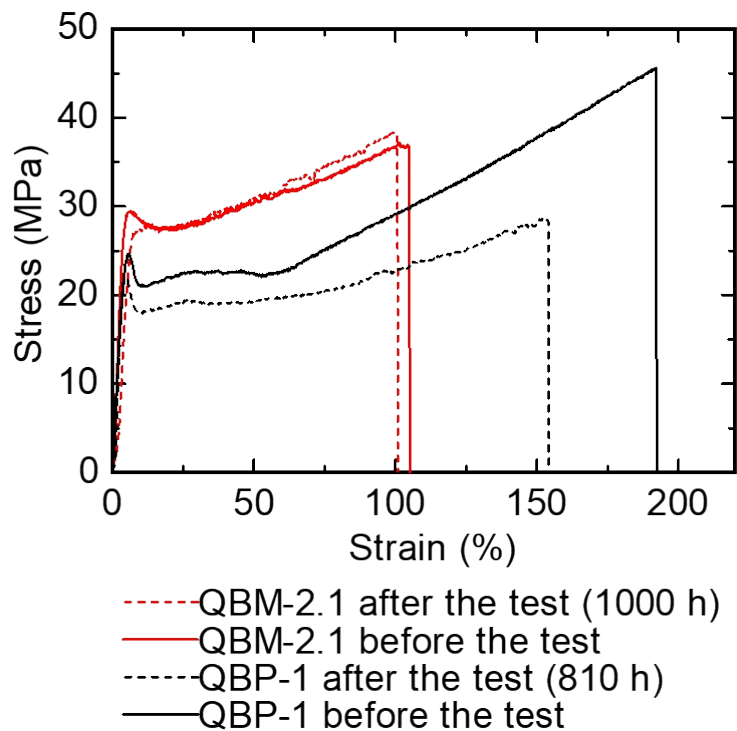


Fig. S9 Stress versus strain curves of QBP-1 and QBM-2.1 before the alkaline stability test (in 8 M KOH at 80 °C) (solid lines) and after the alkaline stability test (dashed line) membranes in Cl<sup>-</sup> forms at 80 °C and 60% RH.

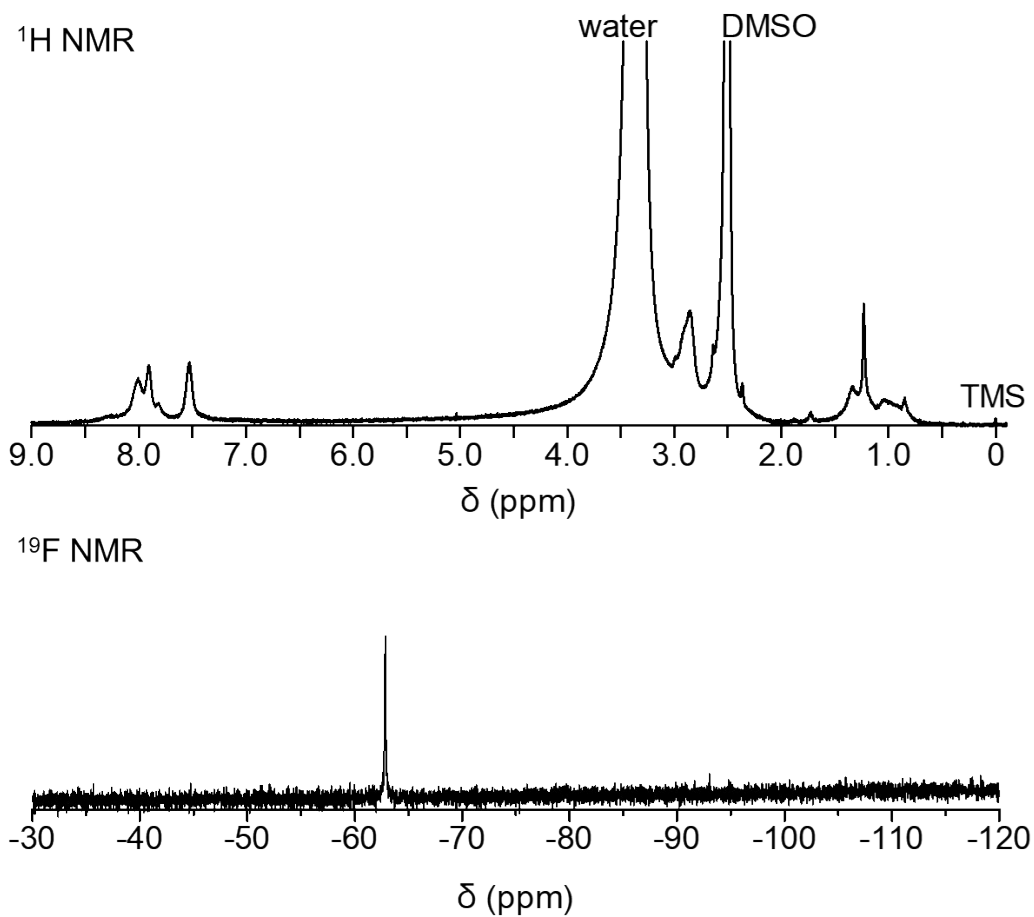


Fig. S10  $^1\text{H}$  and  $^{19}\text{F}$  NMR spectra of QBM-2.7 after the alkaline water electrolysis cell test for 1000 h in  $\text{DMSO-}d_6$ .